Journal of Applied Pharmaceutical Research
Volume 13 Issue 5, Year of Publication 2025, Page 74 – 90
DOI: https://doi.org/10.69857/joapr.v13i5.1188

Check for updates

Research Article

JOURNAL OF APPLIED PHARMACEUTICAL RESEARCH | JOAPR
www.japtronline.com ***ISSN: 2348 – 0335***

DESIGN AND OPTIMIZATION OF CHITOSAN MICROSPHERES LOADED WITH GREEN TEA PHYTOSOMES FOR SUSTAINED RELEASE

Juti Rani Devi[1,2]*, Trishna Das[3], Bhupen Kalita[4], Bhargab Jyoti Sahariah[2]

Article Information
Received: 25th May 2025
Revised: 29th August 2025
Accepted: 18th September 2025
Published: 31st October 2025

Keywords
Microsphere, phytosome, green tea, polyphenols, in vitro washed off.

ABSTRACT

Background: Phytosomes are nanovesicular systems that integrate plant extracts with phospholipids to improve the solubility, stability, and bioavailability of phytoconstituents. Green tea (*Camellia sinensis*) is rich in polyphenols such as epigallocatechin gallate (EGCG) and epigallocatechin (EGC), which possess significant therapeutic potential but are limited by poor absorption and stability. The present study aimed to formulate and evaluate green tea extract–loaded phytosome-incorporated microspheres with desirable physicochemical characteristics for sustained delivery. **Methodology:** Phytosomes were prepared using the thin-layer hydration method with varying molar ratios (0.5–1.0) of phospholipids to standardized green tea extract (sample 1 and sample 2). The optimized phytosomes were further encapsulated into microspheres via emulsion cross-linking, employing different concentrations of glutaraldehyde and polymer to obtain nine formulations. Design Expert software was applied for optimization, and the microspheres were evaluated for micrometric properties, entrapment efficiency, drug loading, drug release, swelling behaviour, mucoadhesion, stability, and surface morphology. **Results and Discussion:** The prepared microspheres exhibited a spherical morphology with satisfactory physicochemical properties. Among the formulations, batch F3 of sample 1 demonstrated the most promising results, achieving 87% yield, 77% drug entrapment efficiency, 30% drug loading, and 91.87% cumulative drug release up to 9 hours, along with favorable swelling and mucoadhesion properties. Stability studies further confirmed the reliability of the formulation. **Conclusion**: Overall, the developed phytosome-loaded microspheres of green tea extract exhibited an improved release profile, stability, and potential fwr sustained drug delivery, suggesting their applicability in enhancing the therapeutic efficacy of green tea polyphenols.

[1]*Assam science and Technology University, Jalukbari, Guwahati, Assam-781013, India*
[2]*Nemcare group of institution, Mirza, Kamrup, Assam- 781125, India*
[3]*Girijananda Choudhury University, Guwahati, Assam-781017, India*
[4]*NEF college of Pharmacy, Lokhra, Guwahati, Assam-781040, India*

For Correspondence: **jutiranidevi@gmail.com**

INTRODUCTION

The development of novel drug delivery systems has garnered significant attention in recent years, aiming to enhance the therapeutic efficacy and bioavailability of poorly soluble phytoconstituents [1,2]. Among these, microspheres containing phytosomes represent a promising approach for improving the stability, absorption, permeation, and controlled release of bioactive plant-derived compounds [3, 4]. Phytosomes are phospholipid-based complexes that enhance the solubility and permeability of phytochemicals, thereby overcoming the limitations associated with conventional herbal formulations.

However, despite their advantages, phytosomes often suffer from stability issues and rapid elimination, which can reduce their therapeutic potential [5–7]. To address these challenges, encapsulation of phytosomes in microspheres has been explored as an advanced strategy to prolong drug retention, protect bioactive compounds from degradation, and provide sustained release properties [8, 9]. Microspheres are spherical, biodegradable carriers with sizes ranging from 1 to 1000 µm, composed of polymers such as chitosan, alginate, and poly(lactic-co-glycolic acid) (PLGA) [10,11].

These carriers effectively encapsulate phytosome complexes, offering multiple advantages, including improved bioavailability, site-specific drug delivery, and reduced toxicity [12, 13]. The combination of phytosomes with microspheres provides a dual enhancement system, where phytosomes improve solubility, and microspheres ensure controlled and targeted release [14, 15]. The integration of phytosomes into microspheres has shown promising applications in the treatment of chronic diseases, including cancer, neurodegenerative disease, and inflammatory conditions [16].

Several studies have demonstrated that phytosomal microspheres significantly enhance the pharmacokinetics and pharmacodynamics of herbal bioactives, making them a viable platform for future therapeutic applications [16–19].

MATERIALS AND METHODS

Materials

Chitosan, glacial acetic acid, ethanol, span 80, liquid paraffin, glutaraldehyde, petroleum ether, acetone (ADVENT CHENBIO PVT. LTD.), prepared phytosomes containing green tea extracts. All chemicals used for this research work were analytical grade.

Methods

Preparation of Microspheres

Microspheres were prepared by the emulsion cross-linking method. A 2% (w/v) chitosan solution was prepared in 4% aqueous glacial acetic acid by overnight stirring in a magnetic stirrer. The required (equivalent) quantities of prepared phytosomes were dissolved in ethanol and thoroughly mixed with the polymer solution. A volume of 6 mL of the above resultant mixture was then injected through a syringe into 40 mL of the oil phase containing Span 80 (7% v/v). Stirring was performed using a mechanical stirrer at 900 rpm to form a water-in-oil emulsion. The oil phase was light-liquid paraffin. After a 30-minute homogenization period, the required volume of 25% glutaraldehyde (v/v) was added slowly. It was then left to stabilize and cross-link. The microspheres obtained were centrifuged, and the sediment was then washed three times with petroleum ether and acetone, followed by drying in a hot air oven at approximately 50°C [20–22]. The composition for the formulation is given in Table 1 below.

Table 1: Formulation of microsphere

Batch	Drug (mg)	Polymer(mg)	Glutaraldehyde(mg)
F1	100	150	0.79
F2	100	100	2
F3	100	200	2
F4	100	150	1.5
F5	100	100	1
F6	100	200	1
F7	100	220.71	1.5
F8	100	150	2.21
F9	100	79.29	1.5

Experimental Design For Optimization

A 2-factor, 3-level factorial design was employed for the formulation of microspheres using Design Expert® software (Version 9, Stat-Ease Inc.). Based on this experimental design, a total of nine runs were executed in a completely randomized sequence. The concentrations of the polymer (X_1) and glutaraldehyde (X_2) served as independent variables, while the percentage of drug release (%DR) and particle size were considered dependent response variables. A p-value of less than 0.05 was regarded as statistically significant. By holding other formulation parameters constant, the selected independent variables (A and B) were studied at three different levels: low (-1), medium (0), and high (+1). Response surface methodology was applied to generate predictive models and response surface plots, which were then utilized to analyse the experimental

outcomes [23–25]. The details of the build information and variables are shown in Tables 2 and 3.

Table 2: Build information

File Version	13.0.5.0		
Study Type	Response Surface	**Subtype**	Randomized
Design Type	Central Composite	**Runs**	9.00
Design Model	Quadratic	**Blocks**	No Blocks
Build Time (ms)	13.00		

Table 3: List of dependent and independent variables (Optimisation Levels)

Independent variable	**Variable level**	
	Low (-1)	High (+1)
Amount of polymer (X_1)	100	200
Amount of Glutaraldehyde (X_2)	1	2
Dependent variables		
Y1 = Particle Size		
Y2 = % Drug release		

Table 4: Experimental Design Runs (for Samples 1 and 2)

Formulation	**Run**	**Factor 1 Polymer (mg)**	**Factor 2 Glutaraldehyde (mg)**	**Response 1 %DR**		**Response 2 Particle size (µm)**	
				Sample1	Sample2	Sample1	Sample2
F1	1	150	0.79	91.87	91.37	19.29	18.79
F2	2	100	2	89.32	88.82	23.38	22.88
F3	**3**	200	2	90.32	89.83	27.11	29.61
F4	4	150	1.5	91.45	90.35	28.99	23.49
F5	5	100	1	93.21	92.71	33.47	32.97
F6	6	200	1	91.25	90.75	13.09	12.59
F7	7	220.71	1.5	89.36	88.86	21.36	20.86
F8	8	150	2.21	89.21	88.71	32.97	32.47
F9	9	79.28	1.5	91.25	90.75	32.65	32.15

**Sample 1 – microspheres containing optimised phytosomes of green tea polyphenols (80% EGCG), *Sample 2 – microspheres containing optimised phytosomes of green tea polyphenols (50% EGC)*

Formulation Optimization: ANOVA was employed to develop an optimized formulation, comparing predicted and actual values of responses for particle size & % drug release.

FTIR: The Fourier transform infrared spectrophotometer was used for FTIR spectroscopy, and the spectra were scanned within the 4000-400 cm-1 wave number range. FTIR study was carried out on drugs enclosed in phytosomes, a physical mixture of phytosome and polymer, Phytosome microspheres.

Micromeritic Properties of Microspheres: For the prepared microspheres, several metrics were assessed, including Hausner's ratio, compressibility index, bulk density, tapped density, and angle of repose.

Determination of Percentage Yield, Drug Loading, and Entrapment Efficiency: A glass mortar and pestle were used to grind a weighed quantity of microspheres equivalent to 10mg of standardized green tea extract. The microspheres were then dispersed in 100 mL of phosphate buffer (pH 6.4) and left overnight to extract the medication. Following centrifugation at 2500 rpm for 10 minutes, the resulting supernatant was diluted with methanol. The absorbance of the solution was subsequently measured at 277 nm—the maximum wavelength (λmax) for polyphenols—using a UV-visible spectrophotometer (Shimadzu UV-1700). The concentration of green tea extract encapsulated within the microspheres was then determined through reference to a previously established standard graph. The percentage entrapment efficiency was measured 3 times for each batch [26, 27]. By using the given equation, the % yield, drug loading, and entrapment efficiency were calculated.

$$\%\ \boldsymbol{yield} = \left(\frac{\boldsymbol{weight\ of\ prepared\ microspheres}}{\boldsymbol{weight\ of\ drug} + \boldsymbol{weight\ of\ polymer\ used}}\right) \times \mathbf{100}$$

$$\boldsymbol{Drug\ Loading} = \frac{\boldsymbol{weight\ of\ green\ tea\ extract\ in\ prepared\ microsphere}}{\boldsymbol{weight\ of\ microspheres}} \times 100$$

$$\boldsymbol{Entrapment\ Efficiency} = \frac{\boldsymbol{Mass\ of\ green\ tea\ extract\ in\ microspheres}}{\boldsymbol{Initial\ Mass\ of\ Drug}} \times 100$$

In vitro drug release

Drug release evaluation was performed using a Franz diffusion cell apparatus (Logan Instruments, New Jersey, India), as this apparatus imitates the nasal cavity and consists of a donor and receptor compartment. A dialysis membrane (cut-off MW 1200) was used, onto which the drug-loaded microspheres were placed.

A microsphere equivalent to 10 mg of the drug was placed on the donor side by dispersing it in simulated nasal fluid. On the other side, the receptor side chamber contained phosphate buffer (pH 7.4), ethanol (1:1) as the release medium. The temperature of the medium was maintained at 37 ± 0.5 °C and continuously stirred with a magnetic bead at 100 rpm. Samples (0.5 mL) were periodically withdrawn and replaced with fresh medium.

The samples were suitably diluted and analyzed using the UV-Vis spectrophotometric method to determine the percentage drug release at various time points. The release kinetic model of the obtained data was performed using zero-order, first-order, Higuchi, and Korsmeyer-Peppas models to calculate the release constant (k) and diffusional release exponent (n) [27,28]

Degree of swelling of microspheres

A pre-weighed quantity of microspheres (100 mg) was introduced into a centrifuge tube containing 10 mL of phosphate buffer solution at pH 6.4. The samples were allowed to hydrate and swell for over 120 minutes. At designated intervals, 60 and 120 minutes, aliquots were subjected to centrifugation at 2000 rpm for 10 minutes. Following centrifugation, the supernatant was carefully removed, and the swollen microspheres were subsequently weighed to evaluate the extent of swelling [26, 27]. The percentage degree of swelling of the microspheres was determined using the equation below:

$$\textbf{Percentage}\ (\%)\ \textbf{of swelling} = \frac{\textbf{Wt} - \textbf{W0}}{\textbf{W0}} \times \textbf{100}$$

Where *Wt represents the weight of the swollen sample at the stipulated time in the simulated fluid, and the initial weight of microparticles before swelling is* W_O.

In-Vitro **Washes Off Test**

The wash-off method, an in vitro adhesion testing technique, was employed to evaluate the mucoadhesive properties of the microspheres. A 1x1 cm piece of pig nasal mucosa was secured with thread onto a glass slide. As the nasal route is the most promising and trending route nowadays, due to its numerous advantages over other routes, and since this research targets mucoadhesive microspheres, the mucin layers of the nasal cavity make mucoadhesive microspheres a preferred formulation for the nasal cavity over other formulations.

The prepared slide was attached to one of the grooves of a USP pill disintegration test device after a weighed quantity of microspheres had been applied to the wet, washed tissue specimen. The disintegrating test apparatus was used, and the tissue sample was periodically moved up and down in the beaker of the disintegrating apparatus, which contained pH 6.4 phosphate buffer.

The drug content of the perfusate was examined after an hour. The difference between the amount of applied and flowing microspheres was used to estimate the number of adhered microspheres [28, 29].

$$\%\ \textbf{Mucoadhesion} = \frac{\textbf{Mass of used sample} - \textbf{mass of detached sample}}{\textbf{Weight of sample}} \times 100$$

Surface Morphology

The microspheres were morphologically characterized using scanning SEM at both greater and lower resolution. Particle size, surface morphology, and texture have all been determined using scanning electron microscopy. Scanning microscopes were used to conduct SEM investigations.

Accelerated Stability Studies

The microspheres' accelerated stability evaluation was performed at 8˚C ± 2.8˚C, 25˚C ± 2˚C/60 % ± 5% RH, and 40˚C ± 2˚C/75 % ± 5% RH. The samples were packaged in polyethylene bottles with child-resistant closures and stored in a stability chamber. The samples were withdrawn at predetermined intervals (0, 1, 2, 3, and 6 months) and evaluated for different parameters [30].

RESULTS AND DISCUSSION

Preparation Of Microspheres

The nine runs from the design expert program were used to create the microspheres utilizing the emulsion cross-linking procedure. A total of 18 runs were obtained for both samples. Various process & formulation-related variables were used during the study, including the concentration of polymer and the amount of glutaraldehyde, and were evaluated for optimization.

Based on the results of particle size and percentage drug release (Table 4) and their statistical analysis, batches F3 and F4 for samples 1 and 2, respectively, are selected as the best formulations. According to the statistical data, the predicted values and actual values are approximately the same for particle size and percentage drug release in formulations F3 and F4, respectively, and can be used for further research [31, 32].

Formulation Optimisation

ANOVA was employed to develop an optimized formulation comparing predicted and actual values of responses for particle size and percentage drug release. In optimization, the F3 and F4 formulations for sample 1 and sample 2, respectively, yield nearly identical values to the predicted values, confirming that these two batches are the optimal formulations for further research. In this study, comparative results such as percentage drug release and swelling index were primarily reported in terms of mean values without detailed statistical interpretation (e.g., p-values) between batches. While this descriptive approach provides an overview of the formulation performance, it limits the strength of conclusions that can be drawn regarding the significance of differences across batches.

The absence of rigorous statistical comparison, such as hypothesis testing, may reduce the ability to differentiate whether observed variations are due to actual formulation effects or experimental variability. Future studies should incorporate appropriate statistical analyses, such as ANOVA or t-tests with p-values, to substantiate the reliability of inter-batch differences and enhance the robustness and scientific validity of the findings (this is a limitation of this work; further study is needed).

In this study design, two levers of polymers are present: the polymer level (chitosan), X_1, and the glutaraldehyde level, X_2. Both influence droplet viscosity, crosslink density, particle surface smoothness, and packing. The F3/F4 settings produced microspheres with lower inter-particle cohesion and tighter packing, reflected by lower Carr's index and Hausner's ratio (e.g., F3: CI ≈ 13.7%, HR ≈ 1.15; F4: CI ≈ 15.5%, HR ≈ 1.18; angles of repose < 35°), hence better flow and compressibility than several other batches. The moderate–to–high chitosan level stabilizes droplets during emulsification (900 rpm, Span-80 7% v/v, 6 mL aqueous phase into 40 mL oil), yielding more spherical and less porous particles.

In contrast, an intermediate crosslinker level (added after 30 min) prevents stickiness without over-hardening, reducing agglomeration and improving bulk/tapped densities. Too little polymer/crosslinker gives fragile/adhesive particles (poor packing), whereas too much can increase brittleness and interlocking (higher CI/HR). ANOVA result also showed X_1–X_2 significantly affect particle size and % release, consistent with the micromeritic improvements seen in F3/F4. One-way ANOVA indicated significant differences among formulations for entrapment efficiency ($F8 = 38.51$, $p < 0.0001$). Tukey's post hoc analysis revealed that batch F6 had significantly higher entrapment efficiency compared to F1, F2, F3, F5, F8, and F9 ($p < 0.05$), while differences with F4 and F7 were not statistically significant. These findings confirm that the optimized polymer-to-crosslinker ratio in F6 provided the most efficient matrix for drug entrapment.

The statistical evaluation reinforced the formulation-dependent differences observed in microsphere performance. ANOVA of entrapment efficiency confirmed highly significant variation among batches ($p < 0.0001$), with Tukey's post hoc test identifying F6 as superior to most other formulations, indicating that its optimized polymer-to-crosslinker ratio provided the most efficient drug entrapment. Similarly, swelling indices at 120 min differed significantly between batches ($p < 0.0001$), with F6 again showing the highest water uptake and expansion, consistent with its structural capacity for controlled release.

In contrast, ANOVA of cumulative drug release values did not reveal significant differences across batches ($p > 0.05$), suggesting that while entrapment and swelling properties varied markedly, the overall release pattern remained comparable, dominated by a diffusion–swelling–controlled zero-order mechanism. Taken together, the results highlight that F6 combined statistically superior entrapment and swelling with a robust, sustained release profile, supporting its designation as the optimized formulation.

FTIR Study

The interaction between the drug and polymer was studied using FTIR spectroscopy. As no such interaction is observed between the drug and the polymer, as shown in Figure 1.

Micromeritic Properties Of Microspheres

The microspheres' excellent flow characteristics demonstrate that they are not clumped together. The tables displayed the values of various parameters for various batches (Tables 5 & 6). The micromeritic properties of the prepared microspheres revealed favorable flowability and packing behavior, which are essential for ensuring uniform dosing and reproducibility during formulation. Bulk and tapped density values suggested uniform particle packing, while Carr's index (13–18%) and Hausner's ratio (1.15–1.22) indicated fair to good flow characteristics.

The angle of repose values (<35°) further confirmed acceptable flowability with minimal inter-particulate friction. These properties are significant for nasal delivery, as smooth flow ensures accurate dosing and facilitates even distribution of microspheres in the nasal cavity. Good flowability also minimizes agglomeration, thereby improving surface contact with the nasal mucosa and enhancing mucoadhesion. Moreover, the micromeritic results support the SEM findings of spherical morphology with smooth surfaces, which are advantageous for deposition, retention in the nasal mucosa & subsequent sustained drug release. Collectively, these parameters confirm that the developed microspheres exhibit suitable micromeritic characteristics for drug delivery applications, especially for nasal delivery.

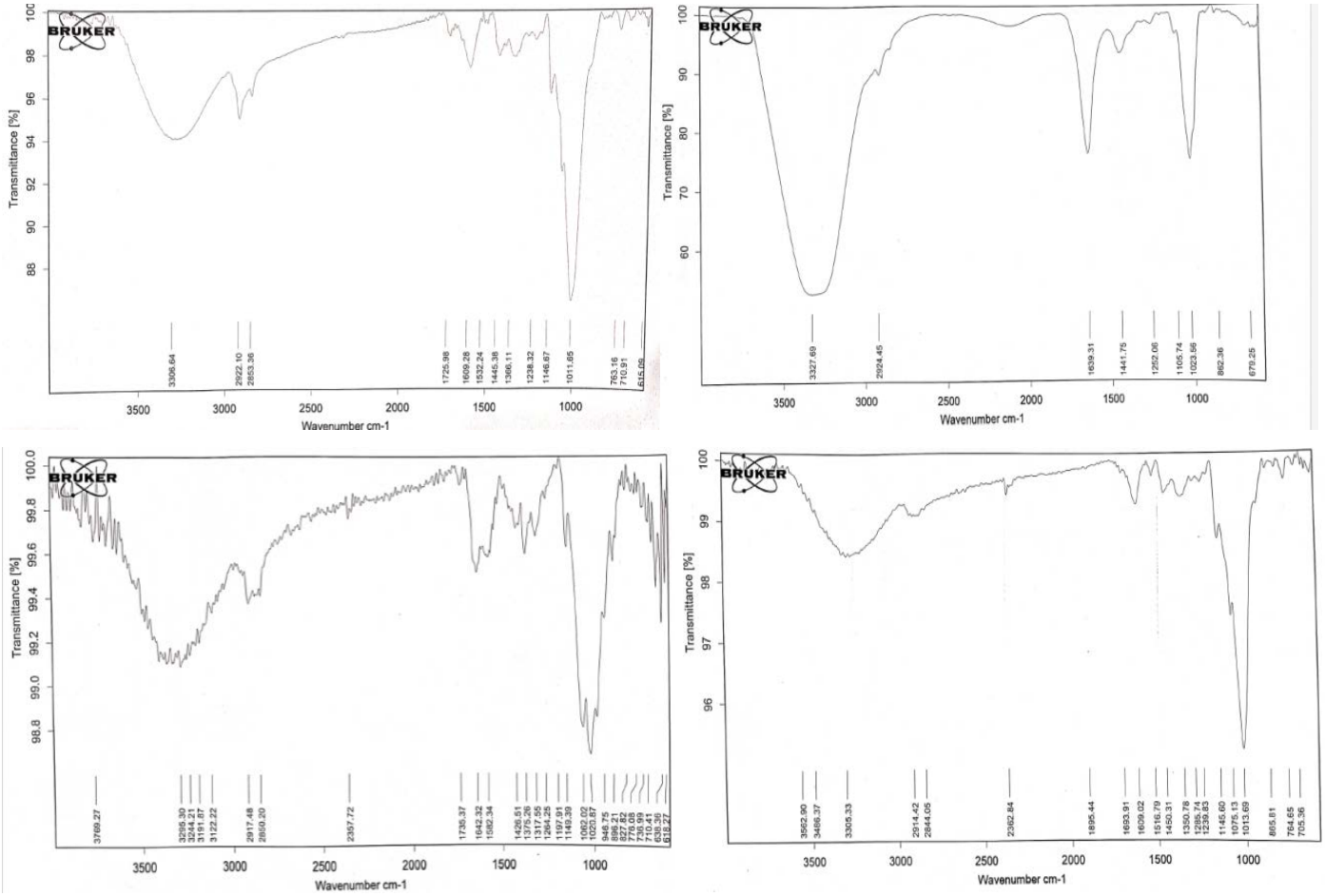

Figure 1: IR spectra of a) phytosomes, b) glutaraldehyde, c) polymers, d) physical mixture of phytosome and polymer

Table 5: Micromeritic Properties of Microspheres (Sample 1)

Batches	Bulk density* (g/cm^3)	Tapped density* (g/cm^3)	Carr's index*	Hausner's ratio*	Angle of Repose* (θ)
F1	0.253±0.0144	0.301±0.0274	15.94±0.37	1.18±0.027	33.59±0.18
F2	0.382±0.0120	0.455±0.0165	16.04±0.23	1.19±0.013	32.61±0.24
F3	0.416±0.0251	0.482±0.0143	13.69±0.28	1.15±0.038	30.78±0.26
F4	0.316±0.0190	0.374±0.0138	15.5±0.19	1.18±0.029	32.63±0.25
F5	0.376±0.029	0.452±0.0235	16.81±0.41	1.20±0.031	27.78±0.14
F6	0.241±0.0131	0.296±0.0179	18.58±0.14	1.22±0.020	30.12±0.28
F7	0.387±0.045	0.442±0.0186	14.5±0.23	1.16±0.039	31.56±0.27
F8	0.395±0.028	0.450±0.0234	17.5±0.12	1.21±0.027	30.59±0.28
F9	0.387±0.026	0.410±0.0224	16.64±0.24	1.16±0.23	30.45±0.21

Table 6: Micromeritics Properties of Microspheres (Sample 2)

Batches	Bulk density (g/cm^3)	Tapped density (g/cm^3)	Carr's index	Hausner's ratio	Angle of Repose (θ)
F1	0.157±0.0124	0.201±0.0254	15.94±0.37	1.18±0.027	33.59±0.18
F2	0.284±0.0210	0.355±0.0262	16.04±0.23	1.19±0.013	32.61±0.24
F3	0.324±0.0251	0.382±0.0273	13.69±0.28	1.15±0.038	30.78±0.26
F4	0.226±0.0170	0.284±0.0238	15.5±0.19	1.18±0.029	32.63±0.25
F5	0.296±0.049	0.372±0.0145	16.81±0.41	1.20±0.031	27.78±0.14
F6	0.246±0.0131	0.299±0.0279	18.58±0.14	1.22±0.020	30.12±0.28
F7	0.277±0.035	0.341±0.0186	14.5±0.23	1.16±0.039	31.56±0.27
F8	0.285±0.038	0.320±0.0134	17.5±0.12	1.21±0.027	30.59±0.28
F9	0.287±0.026	0.315±0.0157	18.6±0.32	1.23±0.038	31.64±0.17

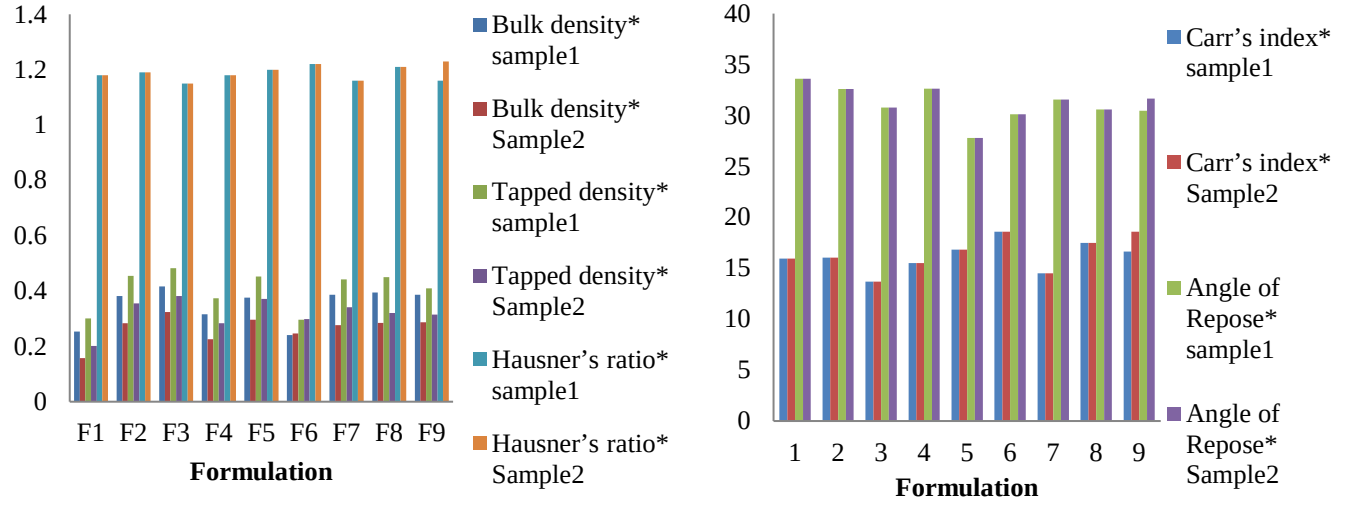

Figure 2: Micromeritics Properties of Microspheres

Determination of % yield, drug loading, entrapment efficiency, and drug release

For sample 1, the percentage yield of F1 to F9 ranged from 83.27% to 87.54%, the percentage of drug entrapment efficiency ranged from 72.76% to 82.86%, and the percentage of drug loading ranged from 29.48% to 32.76%. For sample 2, the percentage yield, percentage drug entrapment efficiency, and percentage drug loading were 81.59% to 84.28%, 72.45% to 79.67%, and 29.48% to 32.76%, respectively. Batch F6 demonstrated the highest drug entrapment efficiency (82.86%), which can be attributed to the interplay between polymer concentration and cross-linker ratio. The high chitosan content (200 mg) increased the viscosity of the dispersed phase during emulsification, thereby reducing drug diffusion into the external oil phase and providing a denser matrix that can hold a larger proportion of the phytosome complex. At the same time, the relatively low glutaraldehyde concentration (1 mg) provided sufficient crosslinking to stabilize the microspheres without causing excessive surface shrinkage or drug expulsion, phenomena commonly associated with higher crosslinker levels. In contrast, batches with lower polymer amounts exhibited insufficient matrix volume to retain the drug. At the same time, those with higher crosslinker concentrations tended to form overly rigid shells, which forced drug leakage. Thus, the superior entrapment efficiency observed in F6 is attributable to the synergistic effect of elevated polymer loading and moderate crosslinking, which together create an optimal matrix architecture for maximum drug retention.

All of the values are displayed in Table 7. The %drug release properties are shown in Figure 3 and indicate sustained release up to 540 minutes, with a range of 89 to 93%. The drug release kinetics are shown in Figures 3 and 4, and the data best fit zero-order kinetics for both samples. The zero-order release profile observed for the optimized microspheres likely arises from a combination of matrix-controlled diffusion and controlled swelling/erosion dynamics that maintain an approximately constant drug-delivery surface over time. In these chitosan microspheres, the phytosome payload is homogeneously entrapped within a relatively dense, cross-linked polymeric

matrix (high entrapment efficiency and SEM showing smooth, non-porous surfaces). High polymer loading increases the dispersed-phase viscosity during formation, resulting in a thicker polymeric network surrounding the phytosomes.

A moderate level of glutaraldehyde crosslinking stabilizes this network without producing brittle shells that cause rapid burst release. Upon exposure to aqueous medium, the matrix swells and forms a hydrated gel layer through which the drug diffuses. Because the swelling & modest surface erosion appear to proceed at rates that compensate for the decrease in concentration gradient, the effective diffusion path & exposed surface area remain relatively constant over the sampling period, which yields an approximation constant (zero-order) release rate.

The Korsmeyer supports this mechanistic conclusion–Peppas exponent (n ≈0.56), which indicates anomalous (non-Fickian) transport where both polymer relaxation(swelling/erosion) & diffusion contribute to release. In short, the interplay of (1) uniform drug distribution, (2) dense but hydrated chitosan matrix from high polymer content, (3) moderated crosslink density that prevents rapid drug expulsion but allows controlled gel formation & (4) smooth, low-porosity particle surfaces that avoid burst pathways collectively produces a release regime approaching zero-order kinetics.

Table 7: Percent Yield, Entrapment Efficiency, Drug Loading (Sample 1 and Sample 2)

Batches	% yield		% Drug entrapment efficiency		% Drug Loading	
	Sample 1	Sample 2	Sample 1	Sample 2	Sample 1	Sample 2
F1	84.52±0.66	82.41±0.33	78.28±0.05	78.28±0.05	29.48±0.05	29.48±0.05
F2	83.79±0.36	81.59±0.25	75.27±0.04	75.27±0.04	30.54±0.01	30.54±0.01
F3	87.54±0.49	84.22±0.63	77.79±0.08	77.79±0.08	30.28±0.04	30.28±0.04
F4	85.32±0.63	84.08±0.64	79.59±0.04	79.59±0.04	31.49±0.03	31.49±0.03
F5	83.27±0.45	82.21±0.24	75.98±0.02	75.98±0.02	29.66±0.07	29.66±0.07
F6	86.08±0.62	83.62±0.32	82.86±0.08	82.86±0.08	32.76±0.03	32.76±0.03
F7	84.72±0.45	82.27±0.25	79.67±0.09	79.67±0.09	30.36±0.02	30.36±0.02
F8	86.97±0.32	84.28±0.32	74.87±0.08	74.87±0.08	31.49±0.03	31.49±0.03
F9	87.23±0.30	82.35±0.33	72.76±0.02	72.45±0.04	31.56±0.02	31.27±0.02

Value expressed as Mean ± SD, n = 3.

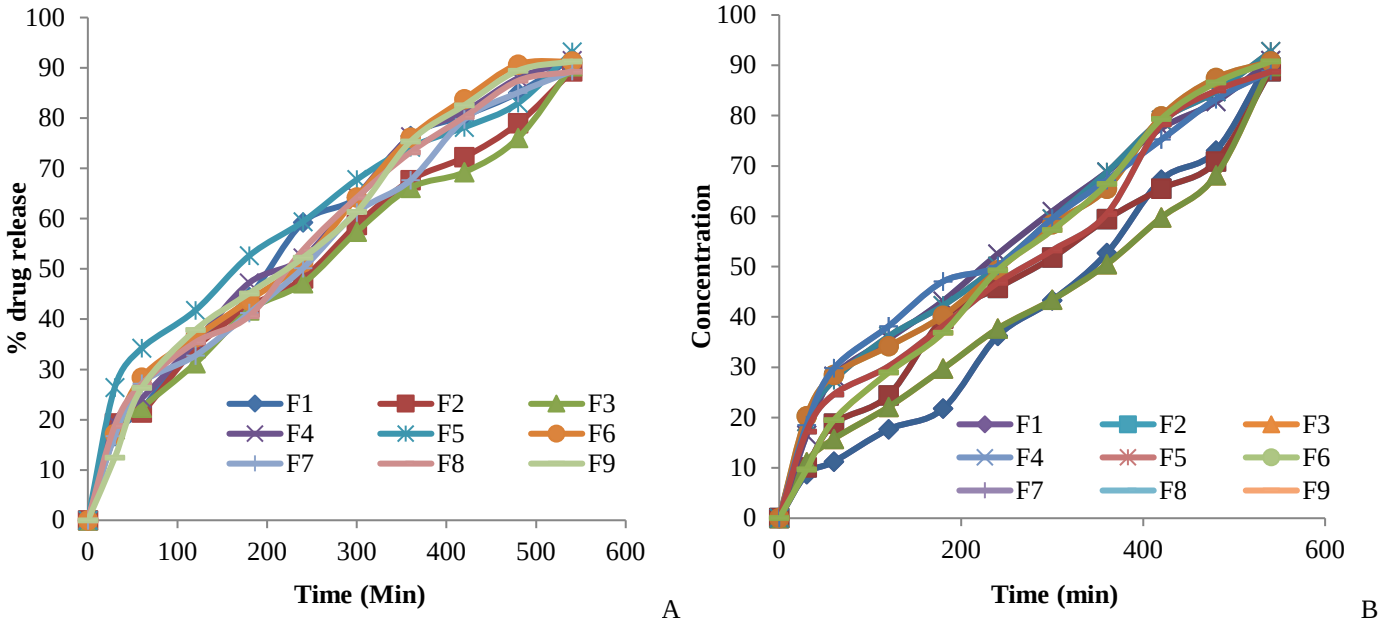

A B

Figure 3: Drug release profile of formulations A. Sample 1, B. Sample 2

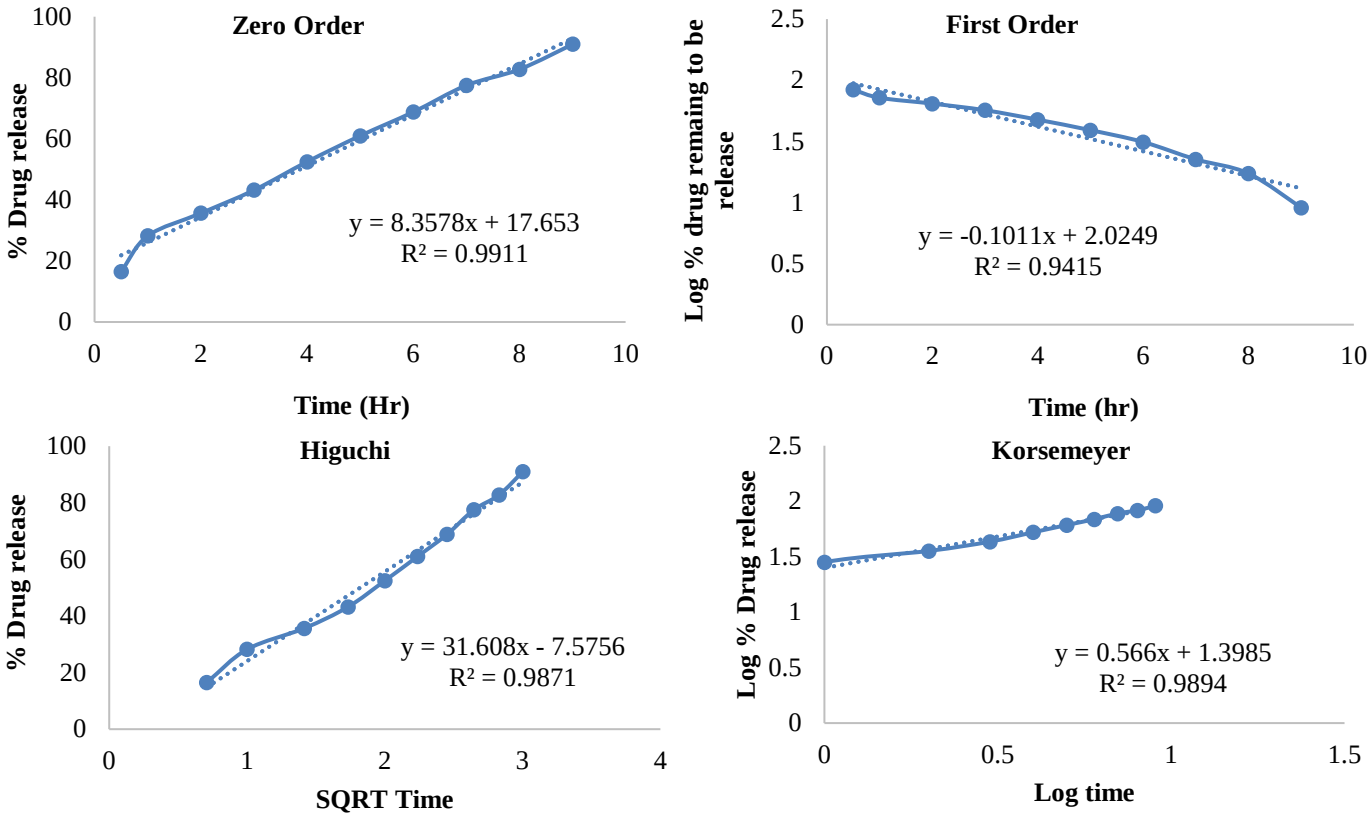

Figure 4: Drug release kinetics for Sample 1

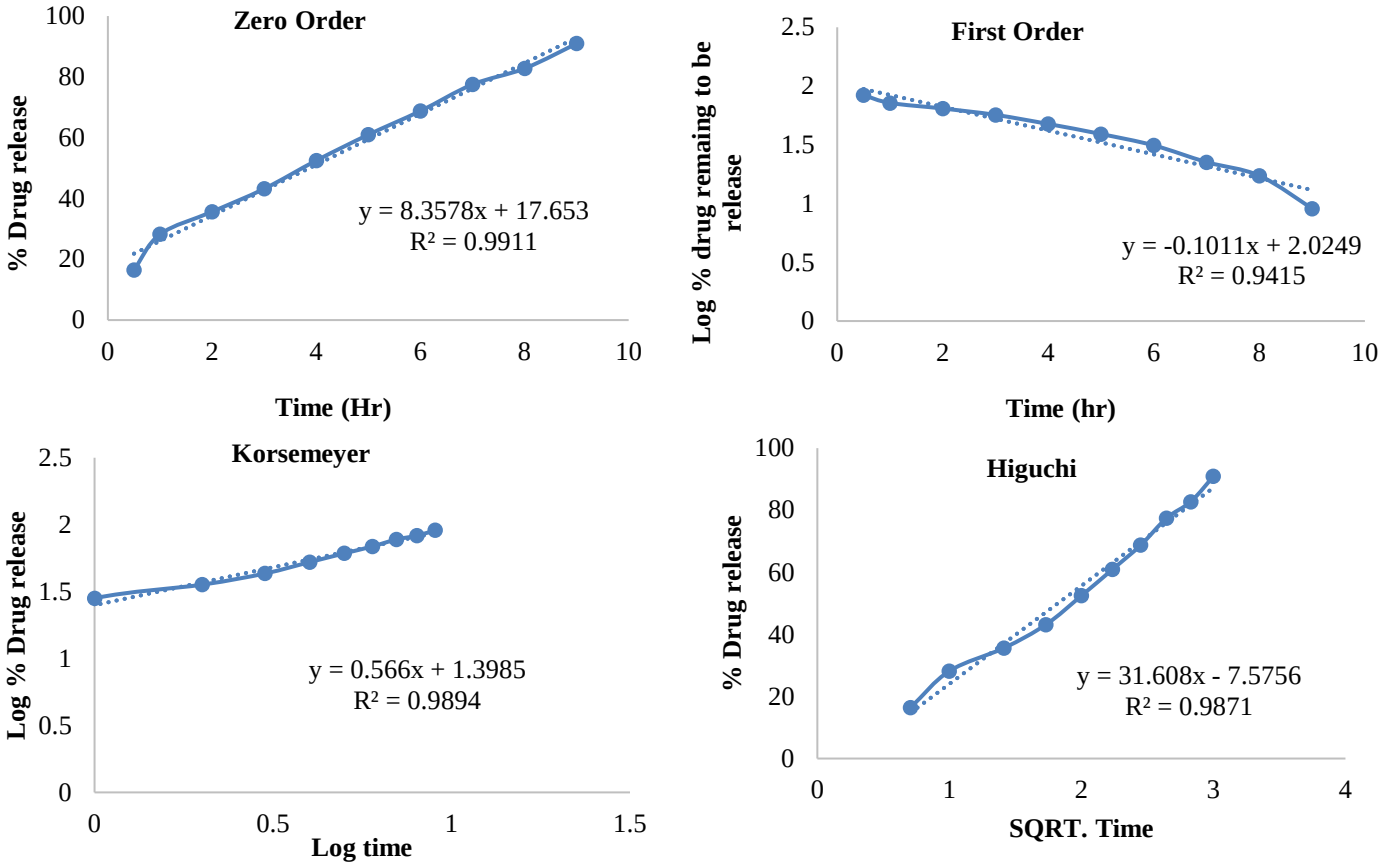

Figure 5: Drug release kinetics for Sample 2

ANOVA: Single Factor (DRUG RELEASE)

SUMMARY

Groups	*Count*	*Sum*	*Average*	*Variance*
78.28	8	616.76	77.095	9.7502
77.26	8	615.43	76.92875	7.086641

ANOVA

Source of Variation	*SS*	*df*	*MS*	*F*	*P-value*	*F crit*
Between Groups	0.11055625	1	0.110556	0.013133	0.910391	4.60011
Within Groups	117.8578875	14	8.418421			
Total	117.9684438	15				

ANOVA: Single Factor (ENTRAPMENT EFFICIENCY)

SUMMARY

Groups	*Count*	*Sum*	*Average*	*Variance*
91.87	8	725.37	90.67125	1.932213
91.37	8	721.38	90.1725	1.931221

ANOVA

Source of Variation	*SS*	*df*	*MS*	*F*	*P-value*	*F crit*
Between Groups	0.99500625	1	0.995006	0.515089	0.484748	4.60011
Within Groups	27.0440375	14	1.931717			
Total	28.03904375	15				

Degree of swelling of microspheres

The phosphate buffer, having a pH of 6.8, easily swelled the prepared microspheres, and all of the produced microspheres quickly expanded. The preparation's polymer composition, crosslinking agent, and crosslinking duration all largely influenced the microsphere's swelling capacity. The amount of polymer has a significant influence on the swelling of microspheres. It has been noted that the swelling property increases with the amount of polymer present [33]. All values are given in Table 8.

Table 8: Swelling index and % mucoadhesion of prepared microspheres

Formulation	**For sample 1**			**For sample 2**		
	% drug swelling at (min)		**% Mucoadhesion**	**% drug swelling at (min)**		**% Mucoadhesion**
	60	**120**		**60**	**120**	
F1	50	90	76.23	45	80	70.47
F2	80	110	86.32	68	97	80.74
F3	60	105	70.47	50	90	69.47
F4	90	140	89.45	73	102	85.43
F5	100	160	84.42	85	110	76.23
F6	140	185	92.65	94	160	88.76
F7	70	150	77.23	65	108	73.21
F8	110	170	90.46	92	140	86.43
F9	85	130	70.67	70	120	68.92

where, number of replicates n = 3

ANOVA: Single Factor (SWELLING INDEX)

SUMMARY

Groups	*Count*	*Sum*	*Average*	*Variance*
90	8	1150	143.75	791.0714
80	8	927	115.875	551.5536

ANOVA

Source of Variation	*SS*	*df*	*MS*	*F*	*P-value*	*F crit*
Between Groups	3108.063	1	3108.063	4.62983	0.04936	4.60011
Within Groups	9398.375	14	671.3125			
Total	12506.44	15				

Batch F6 exhibited the highest swelling index among the formulations, which can be attributed to its high polymer concentration (200 mg chitosan) combined with a relatively low cross-linker concentration (1 mg glutaraldehyde). The higher chitosan content enhanced the hydrophilic nature and water uptake capacity of the microspheres. At the same time, the lower crosslinking density created a less rigid network structure, allowing greater relaxation and expansion of the polymer chains upon hydration. This synergistic effect of increased polymer availability and reduced structural rigidity provided more free volume for water penetration, thereby accounting for the maximum swelling observed in F6.

***In-vitro* wash-off test**

To ensure the formulation adhered to the mucosa at the absorption site for an extended period, a mucoadhesion study was conducted. According to the findings of the in-vitro mucoadhesion investigation, every batch of microspheres exhibited acceptable adhesion and mucoadhesive qualities on the nasal mucosa of sheep. The findings also showed that larger mucoadhesion percentages were attained with increasing polymer ratio and crosslinking speed. This could be attributed to the greater availability of polymer for interaction with mucus [34, 35]. All the values were shown in Table 8.

Surface Morphology

Morphological characterization of the microspheres was carried out by using scanning SEM under higher and lower resolutions. Scanning electron microscopy showed that the microsphere was spherical with a relatively smooth surface, as shown in Figure 6. The prepared microspheres had no holes or ruptures on the surface, which may result in slow clearance and a good deposition pattern in the route of administration, especially in the nasal cavity. The SEM analysis revealed a relatively high surface porosity (~67%) and moderate surface roughness (≈9.9 AU) for the microspheres. The large proportion of porous regions facilitates rapid water penetration and polymer relaxation, while the moderate roughness increases the effective surface area for solvent interaction. Together, these features correlate with the enhanced swelling (highest in F6) and contribute to the sustained yet controlled release profile of the drug. Specifically, the porous structure allows gradual medium uptake and matrix hydration, whereas the absence of deep cracks or ruptures prevents an immediate burst release. So the structural and functional relationship explains the drug release from the microspheres, following a zero-order kinetic model, with consistent diffusion sustained over time.

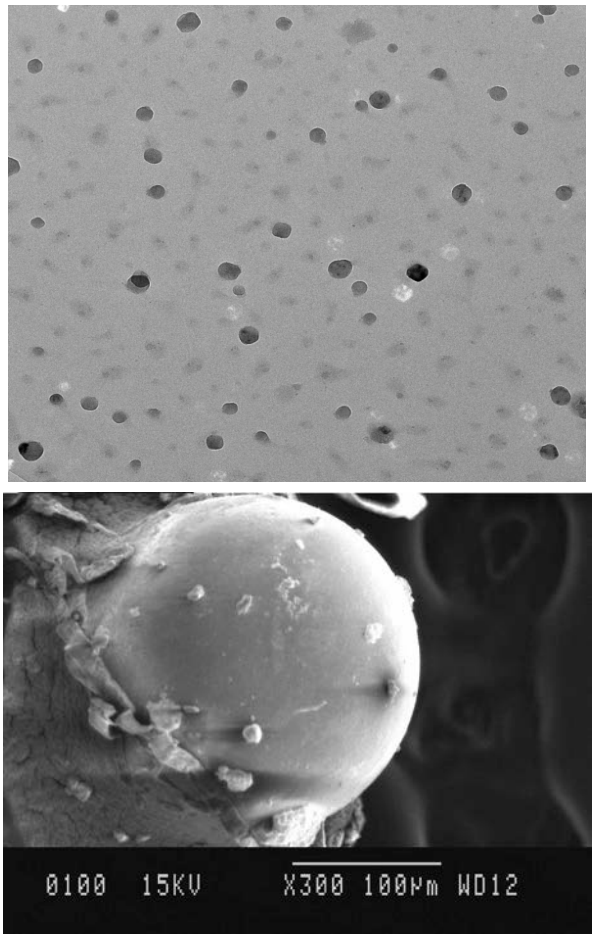

Figure 6: SEM image of microsphere

Accelerated Stability Studies

All stability-related parameters of the microsphere formulations remained within acceptable limits after a 6-month storage period, as presented in Table 9. Throughout the storage period under varying temperature and humidity conditions, no significant changes were observed in the physicochemical properties of the formulations, indicating their stability over time.

STATISTICAL ANALYSIS

Optimisation

The optimization process was carried out by focusing on the percentage of drug release and the particle size of the prepared microspheres. The complete factorial design, including the coded levels of the independent variables along with the corresponding response values, is presented in Table 9. For both samples, the Y1 and Y2 ranges were 13 to 33 µm and 89 to 93% & 12 to 32 µm and 88 to 92%, respectively [36,37]. Design

Expert® (Version 9, Stat-Ease Inc.) was used to simultaneously fit all the answers obtained for the 18 formulations to a variety of models, including first-order, second-order, linear & quadratic models. The results indicate that the 2FI model was the best fit. Table 10 provides a comparison of R2, SD, and CV values. Figure 7 displays the two-dimensional contour plots that were created for each response, whereas Figure 8 displays the three-dimensional response surface plots. These plots are utilized to evaluate the reaction effects between factors on the measured responses. They are particularly effective in assessing the simultaneous influence of two variables on a single response outcome [38-40].

Table 9: stability study of microspheres

Parameters	Initial	1 month	2 months	3 months	6 months
Refrigeration condition (8±2°)					
Appearance	Round	Round	Round	Round	Round
% Drug entrapment efficiency	74.79±0.042	74.66±0.035	74.47±0.022	74.70±0.041	73.42±0.021
% Drug release	91.86	91.87	91.42	91.26	90.62
Room temperature (25±2°/60±5% RH)					
Appearance	Round	Round	Round	Round	Round
% Drug entrapment efficiency	74.79±0.042	74.73±0.041	74.65±0.045	74.27±0.021	74.21±0.067
% Drug release	91.86	91.72	91.27	91.47	90.74
Accelerated condition (40±2°/75±5% RH)					
Appearance	Round	Round	Round	Round	Round
% Drug entrapment efficiency	74.79±0.042	74.79±0.053	74.78±0.022	74.70±0.041	74.22±0.043
% Drug release	91.86	91.64	91.26	90.74	90.43

Table 10: Statistical analysis

For sample1:

Response	R^2	Adj. R^2	Pred. R^2	Adeq.precision	Std. dev.	CV%	Model	
							F Value	P value>F
% Drug release	0.8813	0.8101	0.6166	9.5754	0.5928	0.6528	12.38	0.0095
Particle Size	0.9164	0.8662	0.6665	11.9433	2.64	10.07	18.27	0.0040

For sample2:

Response	R^2	Adj. R^2	Pred. R^2	Adeq.precision	Std.dev.	CV%	Model	
							F Value	P value>F
% Drug release	0.8808	0.8093	0.6143	9.5544	0.5938	0.6575	12.32	0.0096
Particle Size	0.9164	0.8662	0.6665	11.9433	2.64	10.26	18.27	0.0040

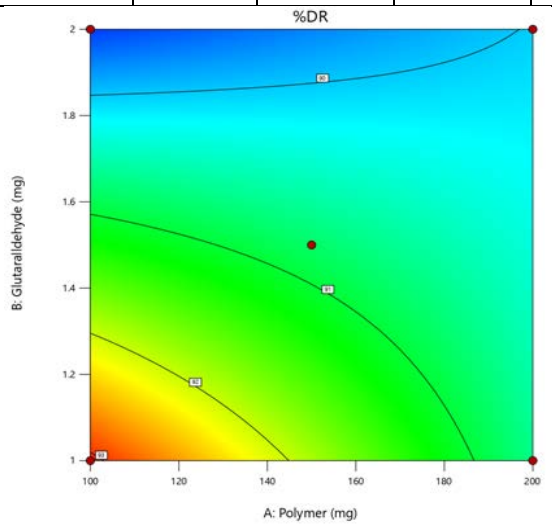

(A)

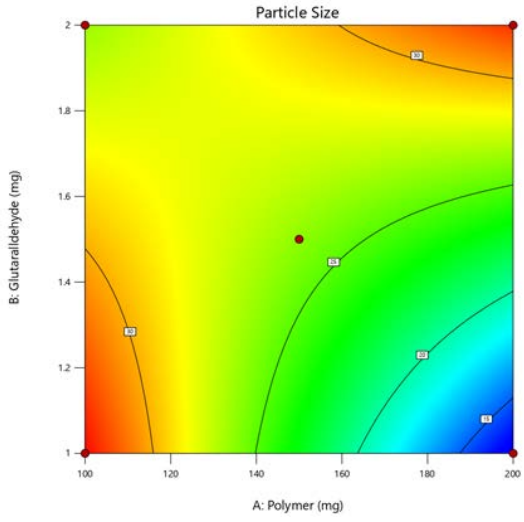

(B)

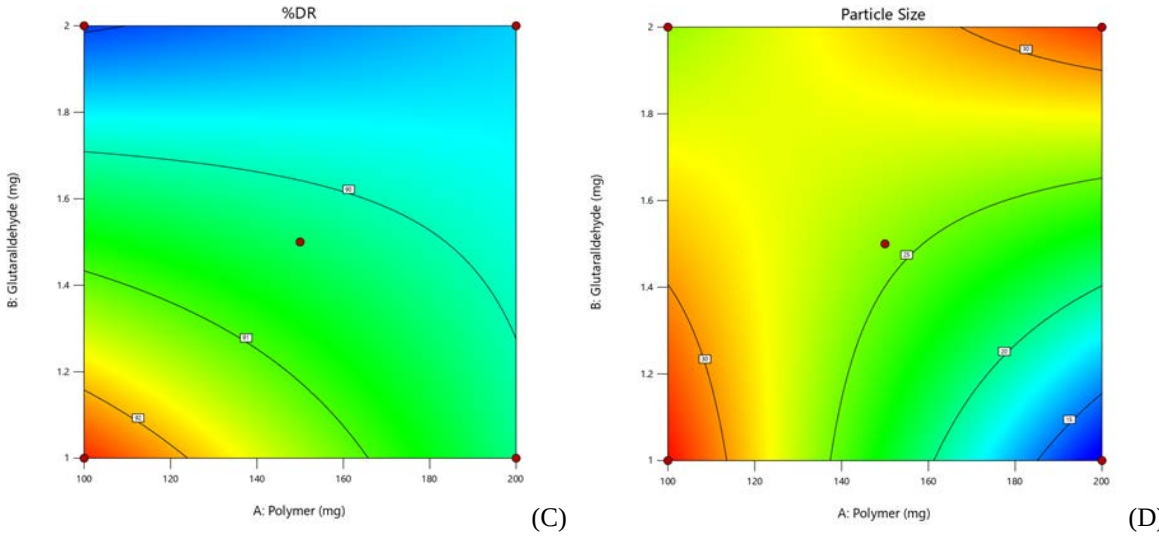

Figure 7: Two-dimensional contour plot for the effect of polymer and glutaraldehyde on % drug release (A), particle size (B) for sample 1, and % drug release (C), particle size (D) for sample 2

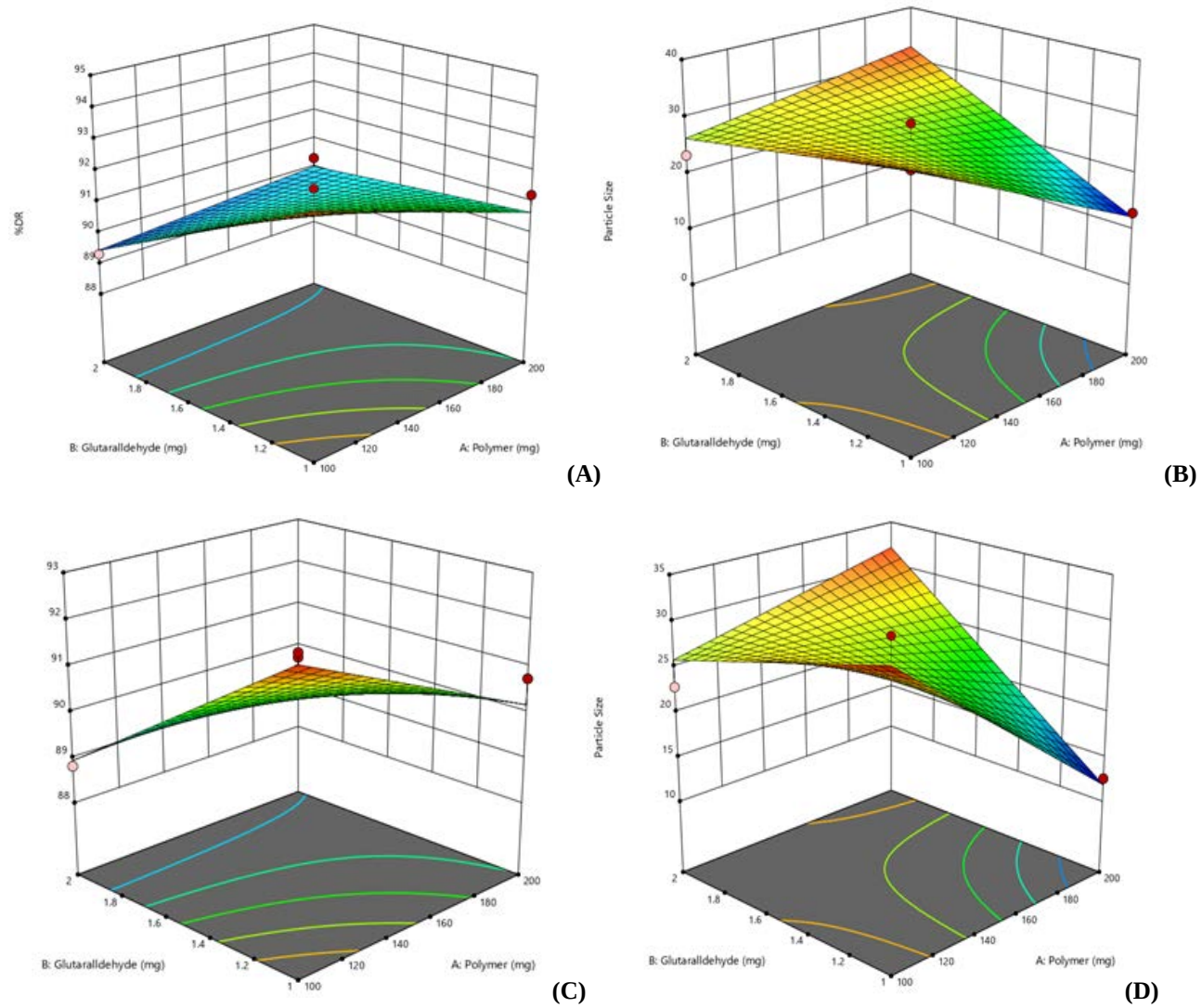

Figure 8: 3D contour plot for the effect of polymer and glutaraldehyde on %drug release (A), particle size (B) for sample 1, and particle size (C), %drug release (D) for sample 2

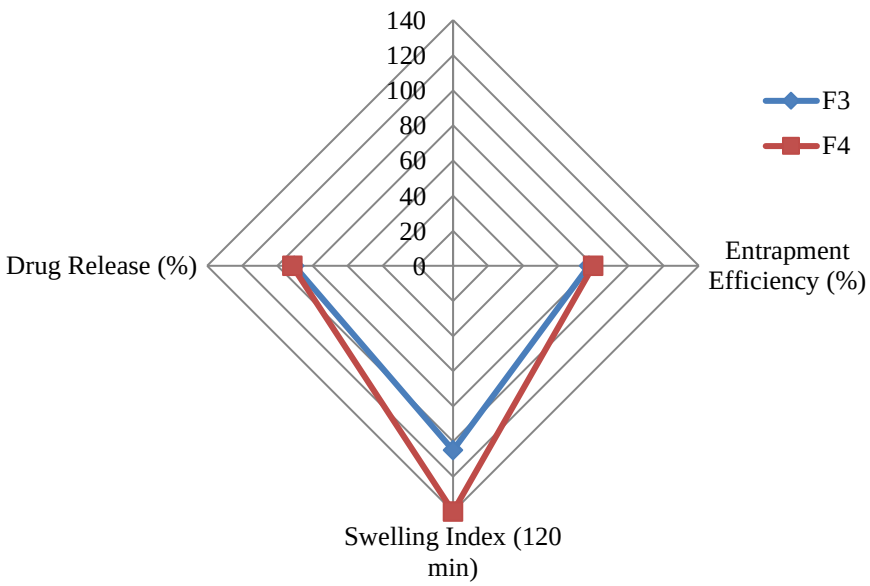

Figure 9: spider plot between F4 & F3

The radar plot (Figure 9) provides a visual comparison of the performance of formulations F3 and F4 across entrapment efficiency, swelling index, and drug release. Both batches exhibited comparable drug release (\~90–91%), suggesting a similar release mechanism. However, F4 demonstrated a clear advantage in swelling index (140 vs 105), indicating higher water uptake and matrix expansion capacity. Entrapment efficiency was also slightly higher for F4 (79.9% vs 77.5%), suggesting improved drug retention during formulation. Overall, the spider chart highlights F4 as the better-performing formulation, with superior entrapment and swelling, while maintaining comparable drug release to F3.

CONCLUSION

In conclusion, it can be summarized that the two different batches of microspheres were prepared successfully with efficient results by enclosing the previously prepared phytosomes loaded with green tea polyphenols (sample 1 and sample 2), and statistically evaluated for various parameters, yielding satisfactory results. As phytosomes stabilise the green tea extract and improve the sustainability of phytosomes, a microsphere formulation was prepared by enclosing the prepared phytosomes. Comparing both formulations, sample 1 (phytosomes containing 80% EGCG), a microsphere formulation, shows better results in all aspects, especially in maintaining sustainability (% drug release) for approximately 90% up to 540 minutes. As the prepared formulation provides a stable form of the herbal extract for a prolonged period, the outcome of the present study suggests the potential application of green tea phytosome-loaded microspheres and the scope for further research in the areas of targeted drug delivery and sustained or controlled drug delivery. The observed interrelationship between micromeritic properties, swelling behavior, and drug release highlights the fundamental role of formulation parameters in dictating the therapeutic performance of phytosome-loaded microspheres. The optimized batch (F3 of Sample 1) not only exhibited superior micromeritic characteristics but also demonstrated enhanced swelling and sustained drug release, underscoring the importance of fine-tuning particle properties for predictable pharmacokinetic outcomes.

These findings extend beyond the present formulation, suggesting that careful modulation of particle size, porosity, and polymeric composition can be strategically employed to design delivery systems with tailored release kinetics. For bioactive compounds like green tea polyphenols, which suffer from poor solubility and instability, this approach offers a practical means of enhancing bioavailability and therapeutic efficacy. Moreover, the demonstrated mucoadhesion and stability of the optimized microspheres position them as promising candidates for oral delivery systems aimed at managing chronic diseases, particularly where prolonged release and consistent plasma levels are desirable. The performance of the optimized microspheres in this study compares favorably with that of previously reported systems designed for the sustained delivery

of phytoconstituents. Earlier studies on green tea extract–loaded chitosan microspheres reported drug entrapment efficiencies in the range of 60–75% and cumulative drug release profiles often characterized by an initial burst followed by a declining release rate, indicative of diffusion-controlled kinetics. The present formulations achieved higher entrapment efficiency (up to 82.86% for F6) and sustained release exceeding 90% over 9 hours with release kinetics best fitting a zero-order model, suggesting superior control over drug release. Similar findings were noted in phytosome-based carriers of EGCG, where incorporation into lipid–polymer hybrid systems improved stability and reduced burst effects; however, incomplete release was often observed within 6–8 hours. Compared with these reports, encapsulation of phytosomes within chitosan microspheres provided a dual advantage: enhanced entrapment due to polymeric matrix stabilization and prolonged release governed by swelling–diffusion interplay. Thus, the present system not only demonstrates improved efficiency and release control over conventional microspheres or phytosome formulations but also highlights its potential as a robust platform for nasal delivery of green tea polyphenols. Earlier studies on green tea extract–loaded chitosan microspheres reported entrapment efficiencies in the range of 60–75% with initial burst release followed by diffusion-driven kinetics [41, 42]. On the other hand, our optimized formulations achieved higher entrapment (up to 82.86%) and sustained zero-order release for 9 h. Similar findings have been reported for EGCG phytosomes, which improved stability but often exhibited incomplete release within 6–8 hours [43, 44]. Compared with these, encapsulation of phytosomes into chitosan microspheres provided both enhanced entrapment and prolonged release [45].

The correlations between formulation parameters provide critical mechanistic insights into the performance of microspheres. A higher drug loading, as observed in batches with greater entrapment efficiency, was generally associated with a more sustained release profile. This can be explained by the denser distribution of drug molecules within the polymeric matrix, which reduced the risk of surface deposition and minimized burst release. Similarly, the swelling index showed a positive relationship with mucoadhesion, as increased water uptake facilitated polymer chain relaxation and enhanced hydrogen bonding with mucin. This suggests that highly swellable formulations, such as F6 and F4, not only allowed greater expansion and diffusion-controlled release but also provided stronger adhesion to mucosal surfaces, potentially prolonging residence time and improving local drug availability. Together, these correlations suggest that formulations with optimized entrapment and swelling properties offer a dual advantage, achieving both controlled drug release and enhanced mucoadhesion, thereby improving therapeutic efficiency.

FINANCIAL ASSISTANCE
NIL

CONFLICT OF INTEREST
The authors declare no conflict of interest.

AUTHOR CONTRIBUTION
Juti Rani Devi performed the studies in the laboratory, recorded observations, and contributed to drafting the manuscript. Trishna Das drafted the manuscript and supervised the manuscript. Bhupen Kalita read and edited the manuscript, and Bhargab Jyoti Sahariah read and finally approved the final manuscript.

REFERENCES
[1] Fayed MH, Alalaiwe A, Almalki ZS, Helal DA. Design Space Approach for the Optimization of Green Fluidized Bed Granulation Process in the Granulation of a Poorly Water-Soluble Fenofibrate Using Design of Experiment. *Pharmaceutics*, **14**, 1471 (2022) https://doi.org/10.3390/pharmaceutics14071471.

[2] Sharma A, Arora K, Mohapatra H, et al. Supersaturation-Based Drug Delivery Systems: Strategy for Bioavailability Enhancement of Poorly Water-Soluble Drugs. *Molecules* **27**, 2969 (2022) https://doi.org/10.3390/molecules27092969

[3] Lazar AR, Puscas A, Tanislav AE, Muresan V. Bioactive compounds delivery and bioavailability in structured edible oils systems. *Compr. Rev. food Sci. food Saf.*, **23**, 1-45 (2024) https://doi.org/10.1111/1541-4337.70020.

[4] Koppula S, Shaik B, Maddi S. Phytosomes as a New Frontier and Emerging Nanotechnology Platform for Phytopharmaceuticals: Therapeutic and Clinical Applications. *Phytother. Res.*, **39**, 2217-2249 (2025) https://doi.org/10.1002/ptr.8465.

[5] Al-Nemrawi NK, Abu Dayah A, Darweesh R. Poly(Lactic-co-Glycolic Acid Nanoparticles Loaded with Docetaxel and Coated with Chitosan, Carboxymethyl Chitosan, or Glycol Chitosan. *Curr. Pharm. Biotechnol.*, 2590 - 2603 (2024) https://doi.org/10.2174/0113892010335722240923110808.

[6] Liu X, Obacz J, Emanuelli G, Chambers JE, Abreu S, Chen X et al. Enhancing Drug Delivery Efficacy Through Bilayer Coating of Zirconium-Based Metal-Organic Frameworks: Sustained Release and Improved Chemical Stability and Cellular Uptake for Cancer Therapy. *Chem. Mater.*, **36**, 3588–3603 (2024) https://doi.org/10.1021/acs.chemmater.3c02954.

[7] Chen W, Li H, Zhang X, Sang Y, Nie Z. Microfluidic preparation of monodisperse PLGA-PEG/PLGA microspheres with controllable morphology for drug release. *Lab Chip*, **24**, 4623-4631 (2024) https://doi.org/10.1039/d4lc00486h.

[8] da Silva AF, Moreira AF, Miguel SP, Coutinho P. Recent advances in microalgae encapsulation techniques for biomedical applications. *Adv. Colloid Interface Sci.*, **333**, 1-9 (2024) https://doi.org/10.1016/j.cis.2024.103297.

[9] Pan CT, Chien ST, Chiang TC, Yen CK, Wang SY, Wen ZH, Yu CY, Shiue YL. Optimization of the spherical integrity for sustained-release alginate microcarriers-encapsulated doxorubicin by the Taguchi method. *Sci. Rep.*, **10**, 21758 (2020) https://doi.org/10.1038/s41598-020-78813-1.

[10] Pandey V, Rathee S, Sen D, Jain SK, Patil UK. Phytovesicular Nanoconstructs for Advanced Delivery of Medicinal Metabolites: An In-Depth Review. *Curr. Drug Targets*, **25**, 847–65 (2024) https://doi.org/10.2174/0113894501310832240815071618.

[11] Park H. Exploring the Effects of Process Parameters during W/O/W Emulsion Preparation and Supercritical Fluid Extraction on the Protein Encapsulation and Release Properties of PLGA Microspheres. *Pharmaceutics*, **16**, 302 (2024) https://doi.org/10.3390/pharmaceutics16030302.

[12] Cholidis P, Kranas D, Chira A, Galouni EA, Adamantidi T, Anastasiadou C, Tsoupras A. Shrimp Lipid Bioactives with Anti-Inflammatory, Antithrombotic, and Antioxidant Health-Promoting Properties for Cardio-Protection. *Mar. Drugs*, **22**, 554 (2024) https://doi.org/10.3390/md22120554.

[13] Chen Y, Tang Y, Li Y, Rui Y, Zhang P. Enhancing the Efficacy of Active Pharmaceutical Ingredients in Medicinal Plants through Nanoformulations: A Promising Field. *Nanomater. (Basel, Switzerland)*, **14**, 1598 (2024) https://doi.org/10.3390/nano14191598.

[14] Permana AD, Utami RN, Courtenay AJ, Manggau MA, Donnelly RF, Rahman L. Phytosomal nanocarriers as platforms for improved delivery of natural antioxidant and photoprotective compounds in propolis: An approach for enhanced both dissolution behaviour in biorelevant media and skin retention profiles. *J. Photochem. Photobiol. B.*, **205**, 111846 (2020) https://doi.org/10.1016/j.jphotobiol.2020.

[15] Kothawade S, Bhange M, Pande VV. Advancements in Phytosomal Therapies for Liver Cancer: A Comprehensive Review. *Curr. Cancer Drug Targets*, **25**, 1066 - 1082 (2024) https://doi.org/10.2174/0115680096319007240703072650.

[16] Rana L, Harwansh RK, Deshmukh R. Recent Updates on Phytopharmaceuticals-Based Novel Phytosomal Systems and Their Clinical Trial Status: A Translational Perspective. *Crit. Rev. Ther. Drug Carrier Syst.*, **42**, 1–54 (2025) https://doi.org/10.1615/CritRevTherDrugCarrierSyst.v42.i1.10.

[17] Yuan Z, Wan Z, Wei P, Lu X, Mao J, Cai Q, Zhang X, Yang X. Dual-Controlled Release of Icariin/Mg(2+) from Biodegradable Microspheres and Their Synergistic Upregulation Effect on Bone Regeneration. *Adv. Healthc. Mater.*, **9**, e2000211 (2020) https://doi.org/10.1002/adhm.202000211.

[18] Zhang Q, Du Y, Yu M, Ren L, Guo Y, Li Q, Yin M, Li X, Chen F. Controlled release of dinotefuran with temperature/pH-responsive chitosan-gelatin microspheres to reduce leaching risk during application. *Carbohydr. Polym.*, **277**, 118880 (2022) https://doi.org/10.1016/j.carbpol.2021.118880.

[19] Sole-Enrech G, Cano-Corres R, Aparicio-Calvente MI, Spataro N. Elimination of lipaemic interference by high-speed centrifugation. *Biochem. medica*, **33**, 10703 (2023) https://doi.org/10.11613/BM.2023.010703.

[20] Ashikhmin A, Piskunov M, Kochkin D, Ronshin F, Chen L. Droplet Microfluidic Method for Estimating the Dynamic Interfacial Tension of Ion-Crosslinked Sodium Alginate Microspheres. *Langmuir*, 15906–15917 (2024) https://doi.org/10.1021/acs.langmuir.4c01940.

[21] Zhou J, Walker J, Ackermann R, Olsen K, Hong JKY, Wang Y, Schwendeman SP. Effect of Manufacturing Variables and Raw Materials on the Composition-Equivalent PLGA Microspheres for 1-Month Controlled Release of Leuprolide. *Mol. Pharm.*, **17**, 1502–15 (2020) https://doi.org/10.1021/acs.molpharmaceut.9b01188.

[22] Gelli R, Mugnaini G, Bolognesi T, Bonini M. Cross-linked Porous Gelatin Microparticles with Tunable Shape, Size, and Porosity. *Langmuir*, **37**, 12781–9 (2021) https://doi.org/10.1021/acs.langmuir.1c01508.

[23] Ramkanth S, Anitha P, Gayathri R, Mohan S, Babu D. Formulation and design optimization of nano-transferosomes using pioglitazone and eprosartan mesylate for concomitant therapy against diabetes and hypertension. *Eur. J. Pharm. Sci. Off. J. Eur. Fed. Pharm. Sci.*, **162**, 105811 (2021) https://doi.org/10.1016/j.ejps.2021.105811.

[24] Tafere C, Yilma Z, Abrha S, Yehualaw A. Formulation, in vitro characterization and optimization of taste-masked orally disintegrating co-trimoxazole tablet by direct compression. *PLoS One*, **16**, e0246648 (2021) https://doi.org/10.1371/journal.pone.0246648.

[25] Zeng H-L, Qiu Q, Fu T-X, Deng A-P, Xie X-Y. Development and optimization of sustained release triptolide microspheres. *PLoS One*, **18**, e0292861 (2023) https://doi.org/10.1371/journal.pone.0292861.

[26] Verberk IM, Nossent EJ, Bontkes HJ, Teunissen CE. Pre-analytical sample handling effects on blood cytokine levels: quality control of a COVID-19 biobank. *Biomark. Med.*, **15**, 987–97 (2021) https://doi.org/10.2217/bmm-2020-0770.

[27] Khan S, Arshad S, Arif A, Tanveer R, Amin ZS, Abbas S, Maqsood A, Raza M, Munir A, Latif A, Habiba M, Afzal M. Trypsin Inhibitor Isolated From Glycine max (Soya Bean) Extraction, Purification, and Characterization. *Dose. Response.*,

20, 15593258221131462 (2022) https://doi.org/10.1177/15593258221131462.

[28] Maclean N, Armstrong JA, Carroll MA, Salehian M, Mann J, Reynolds G, Johnston B, Markl D. Flexible modelling of the dissolution performance of directly compressed tablets. *Int. J. Pharm.*, **656**, 124084 (2024) https://doi.org/10.1016/j.ijpharm.2024.124084.

[29] Chamsai B, Opanasopit P, Samprasit W. Fast disintegrating dosage forms of mucoadhesive-based nanoparticles for oral insulin delivery: Optimization to in vivo evaluation. *Int. J. Pharm.*, **647**, 123513 (2023) https://doi.org/10.1016/j.ijpharm.2023.123513.

[30] González-González O, Ramirez IO, Ramirez BI, O'Connell P, Ballesteros MP, Torrado JJ, Serrano DR. Drug Stability: ICH versus Accelerated Predictive Stability Studies. *Pharmaceutics*, **14**, 2324 (2022) https://doi.org/10.3390/pharmaceutics14112324.

[31] Ullah F, Shah KU, Shah SU, Nawaz A, Nawaz T, Khan KA, Alserihi RF, Tayeb HH, Tabrez S, Alfatama M. Synthesis, Characterization and In Vitro Evaluation of Chitosan Nanoparticles Physically Admixed with Lactose Microspheres for Pulmonary Delivery of Montelukast. *Polymers (Basel).*, **14**, 3564 (2022) https://doi.org/10.3390/polym14173564.

[32] Li Y, Keqi W, Wang G. Evaluating disease similarity based on gene network reconstruction and representation. *Bioinformatics*, **37**, 3579–87 (2021) https://doi.org/10.1093/bioinformatics/btab252.

[33] Akhlaq M, Azad AK, Ullah I, Nawaz A, Safdar M, Bhattacharya T, Uddin ABMH, Abbas SA, Mathews A, Kundu SK, Miret MM, Murthy HCA, Nagaswarupa HP. Methotrexate-Loaded Gelatin and Polyvinyl Alcohol (Gel/PVA) Hydrogel as a pH-Sensitive Matrix. *Polymers (Basel).*, **13**, 2300 (2021) https://doi.org/10.3390/polym13142300.

[34] Kulkarni R, Fanse S, Burgess DJ. Mucoadhesive drug delivery systems: a promising non-invasive approach to bioavailability enhancement. Part I: biophysical considerations. *Expert Opin. Drug Deliv.*, **20**, 395–412 (2023) https://doi.org/10.1080/17425247.2023.2181331.

[35] Zhang Q, Li X, Jasti BR. Role of physicochemical properties of some grades of hydroxypropyl methylcellulose on in vitro mucoadhesion. *Int. J. Pharm.*, **609**, 121218 (2021) https://doi.org/10.1016/j.ijpharm.2021.121218.

[36] Kiss T, Ambrus R, Abdelghafour MM, Zeiringer S, Selmani A, Roblegg E, Budai-Szűcs M, Janovák L, Lőrinczi B, Deák Á, Bernkop-Schnürch A, Katona G. Preparation and detailed characterization of the thiomer chitosan-cysteine as a suitable mucoadhesive excipient for nasal powders. *Int. J. Pharm.*, **626**, 122188 (2022) https://doi.org/10.1016/j.ijpharm.2022.122188.

[37] Jabar A, Madni A, Bashir S, Tahir N, Usman F, Rahim MA, Jan N, Shah H, Khan A, Khan S. Statistically optimized pentazocine loaded microsphere for the sustained delivery application: Formulation and characterization. *PLoS One*, **16**, e0250876 (2021) https://doi.org/10.1371/journal.pone.0250876.

[38] Perveen R, Latif F, Abbas M, Ayub K, Sarfaraz S, Saeed M, Rana S, Al-Rashida M, Nawaz MA, Hameed A. Optimization study and application of box-behnken model for probing eggshell supported transition metals based catalysts to synthesize hydrazone & dihydropyrimidinones. *Sci. Rep.*, **14**, 23270 (2024) https://doi.org/10.1038/s41598-024-74876-6.

[39] Attia MS, Radwan MF, Ibrahim TS, Ibrahim TM. Development of Carvedilol-Loaded Albumin-Based Nanoparticles with Factorial Design to Optimize In Vitro and In Vivo Performance. *Pharmaceutics*, **15**, 1425 (2023) https://doi.org/10.3390/pharmaceutics150514

[40] Miu D-M, Pavaloiu RD, Sha'at F, Vladu M-G, Neagu G, Manoiu V-S, Eremia M-C. Preparation and Optimization of a Polyhydroxyoctanoate-Hydroxyapatite Composite Available to Scaffolds in Implantable Devices. *Molecules*, **30**, 730 (2025) https://doi.org/10.3390/molecules30030730.

[41] Frenț OD, Duteanu N, Teusdea AC, Ciocan S, Vicaș L, Jurca T, Muresan M, Pallag A, Ianasi P, Marian E. Preparation and Characterization of Chitosan-Alginate Microspheres Loaded with Quercetin. *Polymers*, **14**, 490 (**2022)** https://doi.org/10.3390/polym14030490.

[42] Martinez-Ballesta, M, Gil-Izquierdo A, Garcia-Viguera C, Dominguez-Perles R. Nanoparticles and Controlled Delivery for Bioactive Compounds: Outlining Challenges for New "Smart-Foods" for Health. *Foods*, **7,** 72 (2018) https://doi.org/10.3390/foods7050072.

[43] Barani M, Sangiovanni E, Angarano M, Rajizadeh MA, Mehrabani M, Piazza S, Gangadharappa HV, Pardakhty A, Mehrbani M, Dell'Agli M, Nematollahi MH. Phytosomes as Innovative Delivery Systems for Phytochemicals: A Comprehensive Review of Literature. *Int J Nanomedicine*, **16**, 6983-7022 (2021) https://doi.org/10.2147/IJN.S318416.

[44] Guo Y, Luo J, Tan S, Otieno BO, Zhang Z. The applications of Vitamin E TPGS in drug delivery. *Eur J Pharm Sci.* **13**, 49 (2013):175-86 https://doi.org/10.1016/j.ejps.2013.02.006.

[45] P K, R K. Phytosome Technology: A Novel Breakthrough for the Health Challenges. *Cureus*. **30**, 16 (2024) https://doi.org/10.7759/cureus.68180.